Macromolecular Research

Article

DOI 10.1007/s13233-020-8089-x

www.springer.com/13233 pISSN 1598-5032 eISSN 2092-7673

Improvement in Barrier Properties Using a Large Lateral Size of Exfoliated Graphene Oxide

Jinhwa You[1]
Beomjin Oh[1]
Young Soo Yun*[,2]
Hyoung-Joon Jin*[,1]

[1] Department of Polymer Science and Engineering, Inha University, Incheon 22212, Korea
[2] KU-KIST Graduate School of Converging Science and Technology, Korea University, 145 Anam-ro, Seongbuk-gu, Seoul 02841, Korea

Received September 24, 2019 / Revised January 30, 2020 / Accepted February 9, 2020

Abstract: The gas barrier properties of polymers can be improved by reducing gas diffusivity and solubility by using graphene oxide (GO) of various lateral sizes (~3, ~25, ~45 μm). By using GO, the gas diffusion path of the polymer was effectively increased. To reduce the solubility, alkylated GO (AGO) was synthesized by an S_N2 reaction between octyl amine and GO. The hydrophobicity of AGO was confirmed through contact angle measurements, and octylamine on the AGO surface was identified by Fourier-transform infrared spectroscopy and X-ray photoelectron spectroscopy analysis. When GO and AGO with comparatively large lateral size (~45 μm) were homogeneously dispersed in polyvinyl alcohol (PVA) and polyvinylidene chloride (PVDC), respectively, the oxygen transmission rates (OTR) of resulting PVA/GO and PVDC/AGO composite films were significantly reduced. The OTR of PVA/GO composite film reduced from 1.9 × 100 to 5.0 × 10^{-2} cm^3/m^2·day as compared to neat PVA; whereas, the OTR of PVDC/AGO composite film reduced from 1.2 × 100 to 6.8 × 10^{-1} cm^3/m^2·day. In addition, the water vapor transmission rate (WVTR) of the PVDC/AGO composite film remarkably decreased from 1.4 g/m^2·day (neat PVDC) to ~5.5×10^{-1} g/m^2·day, where the lateral size of AGO was insignificant. The WVTR results of PVDC/AGO composite films are in contrast to those for PVA/GO composite films, which did not demonstrate any improvement in WVTR with the addition of GO. Based on the experimental results, it was determined that oxygen permeability and water vapor permeability are more affected by diffusivity and solubility, respectively.

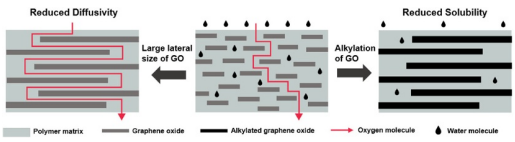

Keywords: Jonscher power law, dielectric relaxation, frequency dependent conductivity, polymer electrolyte membranes.

1. Introduction

Polymers are suitable materials for gas barrier films because of their transparency, flexibility, processability, and lightweight.[1-9] The gas permeability, P of polymers can be expressed as $P = S \times D$, where S is the solubility and D is the diffusivity of gas.[10-13] Thus, reducing the D and S of polymers improves the gas barrier properties. Recently, two-dimensional nanoplatelets such as graphene oxide (GO) and clay have been used as nanofillers to improve the gas barrier properties of polymer nanocomposite films.[4,14-22] The appropriately dispersed nanoplatelets in the polymer matrix extend the diffusion length of the gas molecules through the tortuous effect and reduce gas adhesion and adsorption to the polymer by reducing the S of the polymer.[23-25] Therefore, the lateral size and hydrophobicity of nanoplatelets play an important role in determining the gas barrier properties of polymer nanocomposite films.[19,26,27] Large lateral size nanoplatelets maximize the tortuous effect, effectively reducing the D of the polymer. J. Shen *et al.* prepared a GO-polyether block amide membrane to investigate the size effect of GO on membrane CO_2 gas permeability.[28] P. Das *et al.* used synthetic nanoclays with ultrahigh aspect ratios to improve the gas barrier properties of polyvinyl alcohol (PVA) films.[20] The S of polymer affects the permeability, but most studies have focused on the effect of nanoplatelet size on permeability.[29-33] GO can control the hydrophobicity through various surface modification methods.[8,33,34] Reduced graphene oxide (rGO), produced by chemical reduction with hydrazine, can be used as a filler in high barrier polymer materials because of its hydrophobicity and few defects.[35-40] However, rGO molecules aggregate with each other by strong interaction forces, making it difficult to disperse them homogeneously in organic solvents for polymer fabrication. Alkylation is an effective method of obtaining hydrophobicity and homogeneous dispersion in organic solvents for polymers.[41] J. H. Choe *et al.* prepared alkylated graphene oxide (AGO) using octylamine to ensure the dispersion and hydrophobicity of GO in tetrahydrofuran, a good solvent of polyvinylidene chloride (PVDC).[42] PVDC composite films with AGO showed improved water vapor barrier properties. However, the effect of the lateral size of AGO on the gas barrier properties of PVDC could not be confirmed.

PVA is known as one of the most effective oxygen barrier polymers because of its strong intermolecular forces.[43-46] However, because of the highwater solubility of the hydrophilic functional groups, PVA molecules are swollen and thus lower the water barrier properties.

PVDC has a dense microstructure and strong cohesive energy density because of its head-to-tail structure and low water solubility.[47,48] Therefore, PVDC exhibits excellent oxygen and water vapor barrier properties.[49-52]

Acknowledgments: This research was supported by Inha University Research Grant (2020).

***Corresponding Authors:** Hyoung-Joon Jin (hjjin@inha.ac.kr), Young Soo Yun (c-ysyun@korea.ac.kr)

In this study, we propose an effective method to reduce both *D* and *S* of polymers through GO. The *D* of polymers was controlled by using various lateral sizes (3, 25, and 45 μm) of GO (GO3, GO25, and GO45, respectively), and the *S* of polymers was controlled by hydrophobic AGO prepared using octylamine. Gas barrier properties, including oxygen transmission rate (OTR) and water vapor transmission rate (WVTR), were measured by coating the polymer nanocomposites on poly(ethylene terephthalate) (PET) films based on previously reported studies.[42,53,54] It was found that the OTRs of PVA/GO and PVDC/AGO composite films were reduced as the lateral size of GO increased. The OTR of PVA/GO45 composite film decreased from 1.9×10^{0} to 5.0×10^{-2} $cm^3 m^{-2} day^{-1}$ compared with neat PVA and that of PVDC/AGO45 composite film decreased from 1.2×10^{0} to 6.8×10^{-1} $cm^3 m^{-2} day^{-1}$ compared with neat PVDC. However, the WVTR of PVDC/AGO films ($\sim 5.5 \times 10^{-1}$ $g m^{-2} day^{-1}$) did not depend on the lateral size of AGO. The results of the study show that the permeability of oxygen and water vapor are affected by the *D* and *S* of polymer, respectively.

2. Experimental

2.1. Materials

All GOs with their diverse lateral size were kindly supplied by JMC Corporation (Ulsan, Korea). Octylamine (>99%), PVA (M_w = 85,000 - 234,000, 99% hydrolyzed), 1-methoxy-2-propanol (PGME) (>99.5%), tetrahydrofuran (THF) (>99.5%), and toluene (>99.5%) were purchased from Sigma-Aldrich Chemical Co. (Seoul, Korea). Poly(ethylene terephthalate) (PET, thickness = 125 μm) film coated with polyurethane was purchased from Kolon Co. (Seoul, Korea). Polyvinylidene chloride (PVDC) (M_w = ~90,000) was purchased from Asahi Kasei (Tokyo, Japan).

2.2. Preparation of AGO

Hundred micrograms of GO were dispersed in 50 g of PGME by ultrasonication. Then, 0.5 g of octylamine was added to the GO/PGME solution and stirred at 80 °C for 24 h. The residual octylamine of the AGO/PGME solution was removed using centrifugation at 9500 rpm, 4 °C for 30 min and lyophilized at -50 °C and 0.045 mbar for 72 h using a lyophilizer (LP3, Jouan, France).[41,42]

2.3. Preparation of PVA/GO composite films

Four grams of PVA were dissolved in 50 g of deionized water containing 2 mg of GO by magnetic stirring at 100 °C for 2 h. Subsequently, the resulting PVA/GO nanocomposites were coated on PET films at 60 °C using a wire bar (30). The product was dried in an oven for 12 h at 80 °C (coating thickness = ~2 μm).

2.4. Preparation of PVDC/AGO composite films

Eight grams of PVDC were dissolved in 50 g of the THF/toluene (2:1) mixed solvent containing 16 mg of AGO by magnetic stirring at 60 °C for 30 min. Subsequently, the resulting PVDC/AGO nanocomposites were coated on PET films at 60 °C using a wire bar (7). The product was dried in an oven for 4 h at 80 °C (coating thickness = ~10 μm).

2.5. Characterization

To confirm the dispersion stability of AGO in THF/toluene mixed solvent, a photograph of the nanofillers solutions was obtained using a digital camera (D7200, Nikon, Japan), and the morphologies of GO and AGO were examined using field-emission scanning electron microscopy (FE-SEM, S-4300SE, Hitachi, Japan). Fourier-transform infrared (FT-IR, VERTEX 80 V, Bruker, Germany) spectra of the nanofillers (*i.e.*, GO and AGO) were obtained using an infrared spectrometer in the spectral region of 4000-500 cm^{-1}, over 64 scans with a resolution of 4 cm^{-1}. The chemical compositions of GO and AGO were examined by X-ray photoelectron spectroscopy (XPS, PHI 5700 ESCA, USA) with monochromatic Al Kα radiation ($h\nu$ = 1,486.6 eV). The contact angle images of PVDC, PVA, GO, and AGO were obtained using a digital camera (D7200, Nikon, Japan). Image analyzing software ImageJ and the JAVA plugin were used to determine the contact angle of water droplets resting on the PVDC, PVA, GO, and AGO solid

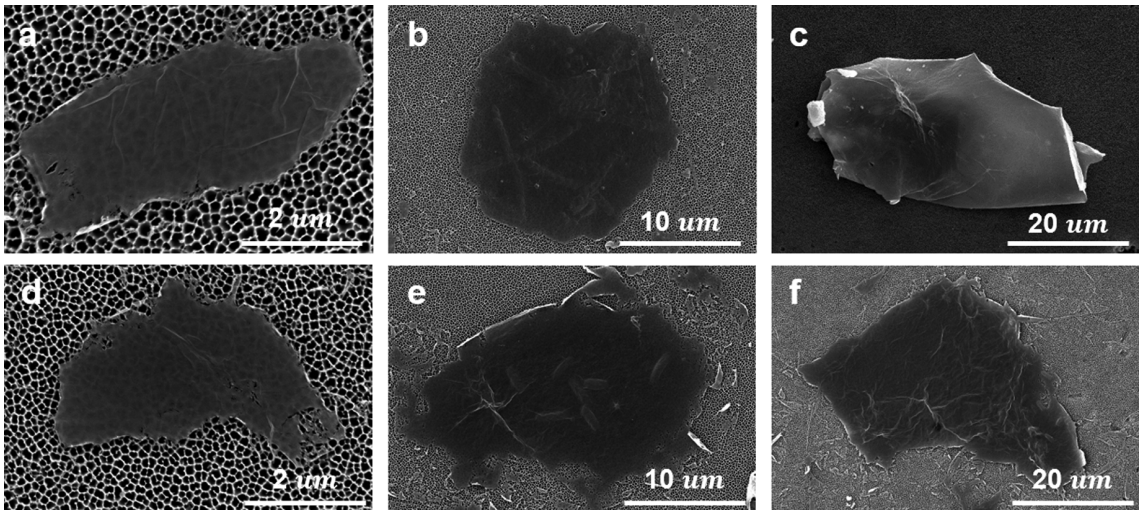

Figure 1. SEM images of (a) GO3, (b) GO25, (c) GO45, (d) AGO3, (e) AGO25, and (f) AGO45.

Table 1. OTR of neat PVA and PVA/GO composite films

Sample	PET film	Neat PVA	PVA/GO3[a]	PVA/GO25[a]	PVA/GO45[a]
OTR ($cm^3\ m^{-2}\ day^{-1}$)	1.6×10^1	1.9×10^0	9.0×10^{-2}	6.0×10^{-2}	5.0×10^{-2}

[a]GO Content (0.05 wt%).

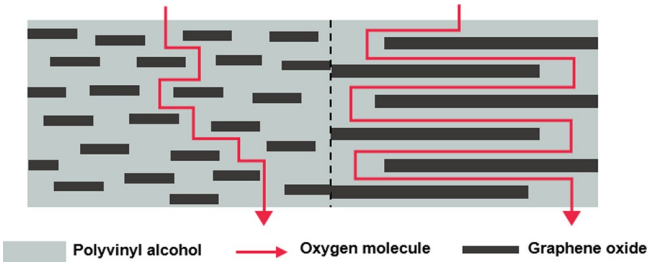

Scheme 1. Gas diffusion path according to lateral size of GO.

surfaces. OTR data were obtained using OX-TRAN Model 2/21 (MOCON, Minneapolis, MN, USA) by ASTM D3985 at 23 °C and 0% RH. WVTR data were obtained using Permatran-W Model 3/61 (MOCON, AQUATRAN2, USA) by ASTM F1249-14 at 38 °C and 100% RH.

3. Results and discussion

3.1. Morphology and lateral size of GO

Well-dispersed GO in polymer forms a tortuous path because of its impermeability.[1,2,35] Therefore, the gas barrier properties of polymer nanocomposite films are affected by the morphology and lateral size of GO. To investigate the morphology and lateral size of GO and AGO, FE-SEM images were obtained (Figure 1). In the FE-SEM images, GO and AGO exhibited a two-dimensional shape with average lateral sizes of ~3, ~25, and ~45 μm (GO3, GO25, and GO45, respectively, and AGO3, AGO25, and AGO45, respectively). In addition, the image did not show significant differences in the morphologies of GO and AGO. This indicates that there is no topology defect in the AGO plane synthesized with octylamine. Thus, GO45 and AGO45 with the largest lateral size were expected to maximize the tortuous effect by effectively extending the gas diffusion path.

3.2. Gas barrier properties of PVA/GO composite coated films

Table 1 shows the OTR of the PVA/GO composite coated on the PET substrate. GO decreased the *D* of PVA by extending the gas diffusion path and reducing the free volume because of hydrogen bonding between GO and PVA. The OTR of the PVA/GO composite films decreased overall compared with that of neat PVA films, and as the lateral size of GO increased, the OTR of the PVA/GO composite films decreased from 9.0×10^{-2} to 5.0×10^{-2} $cm^3\ m^{-2}\ day^{-1}$. These results indicate that a large lateral size of GO can more effectively extend the gas diffusion path of the polymer (Scheme 1). However, because of the water solubility of PVA, the WVTR of PVA/GO could not be measured.

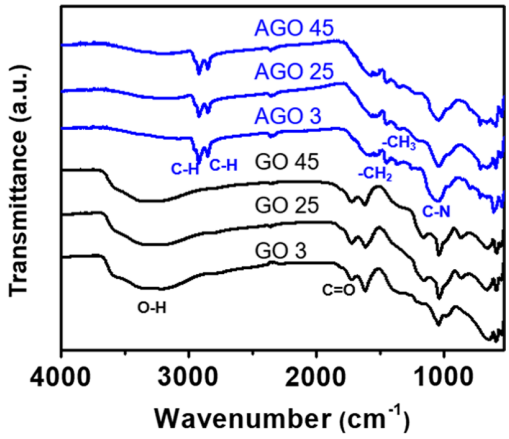

Figure 3. FT-IR spectra of GO3, GO25, GO45, AGO3, AGO25, and AGO45.

Table 2. Carbon, oxygen, and nitrogen contents of GO and AGO calculated by XPS results

Sample	XPS results (at%)		
	C	O	N
GO3	69.8	30.2	-
GO25	67.5	32.5	-
GO45	66.7	33.3	-
AGO3	75.4	20.7	3.9
AGO25	76.8	19.5	3.7
AGO45	75.3	21.0	3.7

3.3. AGO synthesis and characterization

The homogeneous dispersion in the polymer and hydrophobicity of GO are important characteristics because they affect the

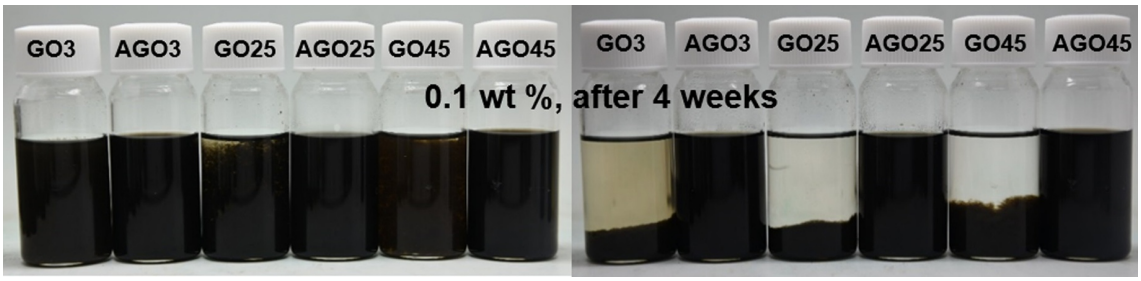

Figure 2. Photographs of dispersion behaviors in THF/toluene (1:2) mixed solution.

Table 3. Contact angle of water on GO, AGO, and PVDC

Sample	Contact angle (°)	Sample	Contact angle (°)
GO3	46.1±1	AGO3	104.0±1
GO25	43.3±1	AGO25	110.2±1
GO45	42.8±3	AGO45	107.8±1
PVA	48.3±2	PVDC	72.6±1

Table 4. OTR and WVTR of neat PVDC and PVDC/AGO composite films

Sample	PET film	Neat PVDC	PVDC/AGO3[a]	PVDC/AGO25[a]	PVDC/AGO45[a]
OTR ($cm^3\ m^{-2}\ day^{-1}$)	1.6×10^1	1.2×10^0	7.5×10^{-1}	6.9×10^{-1}	6.8×10^{-1}
WVTR ($g\ m^{-2}\ day^{-1}$)	5.1×10^0	1.4×10^0	5.5×10^{-1}	5.6×10^{-1}	5.5×10^{-1}

[a]AGO content (0.2 wt%).

improvement in gas barrier properties of polymer nanocomposite films by reducing *D* and *S*. Therefore, various surface modification methods of GO such as reduction with hydrazine and alkylation have been studied to obtain homogeneous dispersion and hydrophobicity of GO in good solvents for polymers. In this study, AGO was synthesized through octylamine because rGO aggregates in THF/toluene mixed solvents, which is a good solvent of PVDC. GO showed unstable dispersion in the THF/toluene mixed solvent, but the prepared AGO showed stable dispersion for four weeks, suggesting homogeneous dispersion in PVDC (Figure 2).

In the FT-IR spectra, the changes in chemical structures of GO and AGO by alkylation were clearly confirmed (Figure 3). C-H related peaks were observed at 2922, 2848, 1457, and 1357 cm^{-1} in AGO spectra, indicating that the alkyl group of octylamine was incorporated on the basal plane of GO. In addition, peaks corresponding to the C-N stretching were observed at 1064 cm^{-1} in AGO spectra.[41,42] The typical broad O-H peak of GO at 3670-2960 cm^{-1} was significantly reduced in the FT-IR spectra of AGO. This change was caused by the alkylation reaction between the octylamine and carboxyl group of GO and the reduction of GO because of the reaction temperature.

To confirm the existence of the amine group on the surface of AGO, the chemical composition ratios of GO and AGO were calculated by XPS analysis (Table 2). AGO3, AGO25, and AGO45 contain 3.9, 3.7, and 3.7 at% nitrogen atoms, respectively, while GO does not contain nitrogen. In addition, the oxygen atoms in AGO were reduced by approximately 10 at% than in GO. The reduced oxygen content of AGO and the introduction of ~3.9 at% nitrogen indicate the introduction of octylamine in AGO, which supplements the FT-IR results (Figure 3).

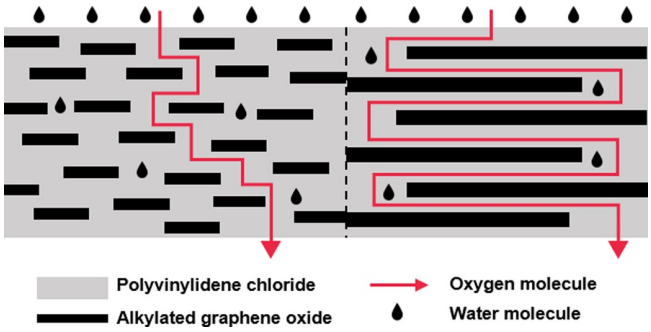

Scheme 2. Gas diffusion path and adhesion and adsorption of water molecule according to lateral size of AGO.

The contact angles were measured to confirm the changes in hydrophobicity of AGO because of the octyl group on the surface of AGO (Table 3). The contact angles for water droplets on AGO3, AGO25, and AGO45 were increased from 46.1, 43.3, and 42.8° to 104.0, 110.2, and 107.8°, respectively, compared with those of GO3, GO25 and GO45, which indicate increased hydrophobicity of AGO. In addition, the contact angle of AGO is larger than that of PVDC (72.6°), which means that the hydrophobicity of AGO is higher than that of PVDC. Therefore, the well-dispersed hydrophobic AGO in PVDC is expected to reduce the *S* of PVDC/AGO composite films.

3.4. Gas barrier properties of PVDC/AGO composite coated films

Table 4 shows the OTRs and WVTRs of PVDC/AGO composites coated on PET substrates. The OTR of the PVDC/AGO composite films decreased linearly from 7.5×10^{-1} to 6.8×10^{-1} $cm^3\ m^{-2}\ day^{-1}$ as the lateral size of AGO increased. This result showed the same trend as the OTR of PVA/GO composite films, which clearly demonstrates that the lateral size of GO affects the *D* of polymers. The WVTR of the PVDC/AGO45 composite film was reduced from 1.4×10^0 to 5.5×10^{-1} $g\ m^{-2}\ day^{-1}$ compared with that of the neat PVDC film, confirming the effect of AGO hydrophobicity. However, the WVTR of PVDC/AGO3 and PVDC/AGO25 composite films were 5.5×10^{-1} and 5.6×10^{-1} $g\ m^{-2}\ day^{-1}$, respectively, which are similar to that of the PVDC/AGO45 composite film. This was probably because water permeability is more dependent on solubility *S* than diffusivity *D*. Unlike oxygen molecules, water molecules absorbed in the polymer reduce barrier properties because they increase the free volume of the polymer by swelling the polymer. High solubility in water promotes the adhesion and absorption of water molecules in the polymer. Therefore, regardless of the lateral size of AGO, similar WVTR values of the PVDC/AGO composite films can be explained by the similar solubilities of AGO3, AGO25, and AGO45 obtained through contact angles (Scheme 2, Table 3).

4. Conclusions

To reduce the *D* of polymers, the gas diffusion path was extended using large lateral size GO, and to reduce the *S* of polymers, the

hydrophobicity of GO was increased by alkylation. The contact angles of the prepared AGO3, AGO25, and AGO45 were 104.0, 110.2, and 107.8°, respectively, which showed similar hydrophobicity. Furthermore, octylamine on the AGO surface was identified by FT-IR and XPS analysis. The gas barrier properties were evaluated by fabricating the PVA/GO and PVDC/AGO composite films. As the lateral size of GO increased from ~3 μm to ~45 μm, the OTR of the PVA/GO composite films decreased from 9.0×10^{-2} to 5.0×10^{-2} $cm^3 m^{-2} day^{-1}$ and the OTR of the PVDC/AGO composite films also decreased from 7.5×10^{-1} to 6.8×10^{-1} $cm^3 m^{-2} day^{-1}$, which was similar to the PVA/GO composite films. However, the WVTR of the PVDC/AGO composite films decreased as compared with neat PVDC; however, it remained almost constant at 5.6×10^{-1} $g m^{-2} day^{-1}$ regardless of the AGO lateral size. This is because the oxygen permeability is more affected by *D*, whereas water vapor permeability is more affected by *S*.

References

(1) K. Choi, S. Nam, Y. Lee, M. Lee, J. Jang, S J. Kim, Y. J. Jeong, H. Kim, S. Bae, J.-B. Yoo, S. M. Cho, J.-B. Choi, H. K. Chung, J.-H. Ahn, C. E. Park, B. H. Hong, *ACS. Nano*, **9**, 5818 (2015).
(2) M. T. Maldonado, O. Martín, M. González, J. Pozuelo, B. Serrano, J. C. Cabanelas, S. M. Vega-Díaz, and J. Baselga, *Adv. Mater.*, **23**, 5302 (2011).
(3) M. Alexandre and P. Dubois, *Mater. Sci. Eng. R: Reports*, **28**, 1 (2000).
(4) J. S. Bunch, S. S. Verbridge, J. S. Alden, A. M. van der Zande, J. M. Parpia, H. G. Craighead, and P. L. McEuen, *Nano Lett.*, **8**, 2458 (2008).
(5) M. Ulbricht, *Polymer*, **47**, 2217 (2006).
(6) S. Sinha Ray, K. Yamada, M. Okamoto, and K. Ueda, *Polymer*, **44**, 857 (2003).
(7) H. Kim, A. A. Abdala, and C. W. Macosko, *Macromolecules*, **43**, 6515 (2010).
(8) H. Kim, Y. Miura, and C. W. Macosko, *Chem. Mater.*, **22**, 3441 (2010).
(9) J.-H. Seok, S. H. Kim, S. M. Cho, G.-R. Yi, and J. Y. Lee, *Macromol. Res.*, **26**, 1257 (2018).
(10) B. Tan and N. L. Thomas, *J. Membr. Sci.*, **514**, 595 (2016).
(11) B. D. Freeman, *Macromolecules*, **32**, 375 (1999).
(12) S. G. Charati and S. A. Stern, *Macromolecules*, **31**, 5529 (1998).
(13) T.-S. Chung, L. Y. Jiang,, Y. Li, and S. Kulprathipanja, *Prog. Polym. Sci.*, **32**, 483 (2007).
(14) D. A. Dikin, S. Stankovich, E. J. Zimney, R. D. Piner, G. H. B. Dommett, G. Evmenenko, S. T. Nguyen, and R. S. Ruoff, *Nature*, **448**, 457 (2007).
(15) Y.-H. Yang, L. Bolling, M. A. Priolo, and J. C. Grunlan, *Adv. Mater.*, **25**, 503 (2013).
(16) H. W. Kim, H. W. Yoon, S.-M. Yoon, B. M. Yoo, B. K. Ahn, Y. H. Cho, H. J. Shin, H. Yang, U. Paik, S. Kwon, J.-Y. Choi, and H. B. Park, *Science*, **342**, 91 (2013).
(17) K.-H. Lee, J. Hong, S. J. Kwak, M. Park, and J. G. Son, *Carbon*, **83**, 40 (2015).
(18) M. A. Priolo, D. Gamboa, K. M. Holder, and J. C. Grunlan, *Nano Lett.*, **10**, 4970 (2010).
(19) G. Choudalakis and A. D. Gotsis, *Eur. Polym. J.*, **45**, 967 (2009).
(20) P. Das, J.-M. Malho, K. Rahimi, F. H. Schacher, B. Wang, D. E. Demco, and A. Walther, *Nat. Commun.*, **6**, 5967 (2015).
(21) K. Takahashi, R. Ishii, T. Nakamura, A. Suzuki, T. Ebina, M. Yoshida, M. Kubota, T. T. Nge, and T. Yamada, *Adv. Mater.*, **29**, 1606512 (2017).
(22) P. Maiti, K. Yamada, M. Okamoto, K. Ueda, and K. Okamoto, *Chem. Mater.*, **14**, 4654 (2002).
(23) J. Wang, D. J. Gardner, N. M. Stark, D. W. Bousfield, M. Tajvidi, and Z. Cai, *ACS Sustain. Chem. Eng.*, **6**, 49 (2018).
(24) A. K. Pal and V. Katiyar, *Biomacromolecules*, **17**, 2603 (2016).
(25) J. M. Lagaron, R. Catalá, and R. Gavara, *Mater. Sci. Technol.*, **20**, 1 (2004).
(26) C. Lu and Y.-W. Mai, *Phys. Rev. Lett.*, **95**, 088303 (2005).
(27) R. K. Bharadwaj, *Macromolecules*, **34**, 9189 (2001).
(28) J. Shen, M. Zhang, G. Liu, K. Guan, and W. Jin, *AIChE J.*, **62**, 2843 (2016).
(29) Y.-H. Yu, C.-Y. Lin, J.-M. Yeh, W.-H. Lin, *Polymer*, **44**, 3553 (2003).
(30) S. Takahashi, H. A. Goldberg, C. A. Feeney, D. P. Karim, M. Farrell, K. O'Leary, and D. R. Paul, *Polymer*, **47**, 3083 (2006).
(31) J. Yu, K. Ruengkajorn, D.-G. Crivoi, C. Chen, J.-C. Buffet, and D. O'Hare, *Nat. Commun.*, **10**, 1 (2019).
(32) C.-N. Wu, T. Saito, S. Fujisawa, H. Fukuzumi, and A. Isogai, *Biomacromolecules*, **13**, 1927 (2012).
(33) C. Xiang, P. J. Cox, A. Kukovecz, B. Genorio, D. P. Hashim, Z. Yan, Z. Peng, C.-C. Hwang, G. Ruan, E. L. G. Samuel, P. M. Sudeep, Z. Konya, R. Vajtai, P. M. Ajayan, and J. M. Tour, *ACS Nano*, **7**, 10380 (2013).
(34) R. K. Layek, A. K. Das, M. J. Park, N. H. Kim, and J. H. Lee, *Carbon*, **81**, 329 (2015).
(35) Y. Su, V. G. Kravets, S. L. Wong, J. Waters, A. K. Geim, and R. R. Nair, *Nat. Commun.*, **5**, 4843 (2014).
(36) K. Goh, J. K. Heising, Y. H. Yuan, H. E. Karahan, L. Wei, S. Zhai, J.-X. Koh, N. M. Htin, F. Zhang, R. Wang, A. G. Fane, M. Dekker, F. Dehghani, and Y. Chen, *ACS Appl. Mater. Interfaces*, **8**, (2016).
(37) T. Kim, J. H. Kang, S. J. Yang, S. J. Sung, Y. S. Kim, and C. R. Park, *Energy Environ. Sci.*, **7**, 3403 (2014).
(38) S. Huang, M. Dakhchoune, W. Luo, E. Oveisi, G. He, M. Rezaei, J. Zhao, D. T. L. Alexander, A. Züttel, M. S. Strano, and K. V. Agrawal, *Nat. Commun.*, **9**, 2632 (2018).
(39) J. Kim, S. H. Song, H.-G. Im, G. Yoon, D. Lee, C. Choi, J. Kim, B.-S. Bae, K. Kang, and S. Jeon, *Small*, **11**, 3124 (2015).
(40) H. Yamaguchi, J. Granstrom, W. Nie, H. Sojoudi, T. Fujita, D. Voiry, M. Chen, G. Gupta, A. D. Mohite, S. Graham, and M. Chhowalla, *Adv. Energy Mater.*, **4**, 1300986 (2014).
(41) M. Y. Song, S. Y. Cho, N. R. Kim, S.-H. Jung, J.-K. Lee, Y. S. Yun, and H.-J. Jin, *Carbon*, **108**, 274 (2016).
(42) J. H. Choe, Y. S. Yun, and H.-J. Jin, *Polym. Korea*, **42**, 377 (2018).
(43) J. Wang, Q. Cheng, L. Lin, L. Chen, and L. Jiang, *Nanoscale*, **5**, 6356 (2013).
(44) J.-T. Chen, Y.-J. Fu, Q.-F. An, S.-C. Lo, Y.-Z. Zhong, C.-C. Hu, K.-R. Lee, and J.-Y. Lai, *Carbon*, **75**, 443 (2014).
(45) J.-H. Yeun, G.-S. Bang, B. J. Park, S. K. Ham, and J.-H. Chang, *J. Appl. Polym. Sci.*, **101**, 591 (2006).
(46) C. Maes, W. Luyten, G. Herremans, R. Peeters, R. Carleer, and M. Buntinx, *Polym. Rev.*, **58**, 209 (2018).
(47) J. L. McClanahan and S. A. Previtera, *J. Polym. Sci. Part A*: *General Papers*, **3**, 3919 (1965).
(48) T. Takahagi, Y. Chatani, T. Kusumoto, and H. Tadokoro, *Polym. J.*, **20**, 883 (1988).
(49) C. Habel, M. Schöttle, M. Daab, N. J. Eichstaedt, D. Wagner, H. Bakhshi, S. Agarwal, M. A. Horn, and J. Breu, *Macromol. Mater. Eng.*, **303**, 1800333 (2018).
(50) M. D. Steven and J. H. Hotchkiss, *Packag. Technol. Sci.*, **15**, 17 (2002).
(51) L. Bastarrachea, S. Dhawan, and S. S. Sablani, *Food Eng. Rev.*, **3**, 79 (2011).
(52) S. Galus and J. Kadzińska, *Polym. Eng. Sci.*, **59**, E375 (2019).
(53) J. H. Choe, J. Jeon, M. E. Lee, J. J. Wie, H.-J. Jin, and Y. S. Yun, *Nanoscale*, **10**, 2025 (2018).
(54) M. E. Lee and H.-J. Jin, *J. Nanosci. Nanotechnol.*, **15**, 10 (2015).

